



Hybrid position/force output feedback second-order sliding mode control for a prototype of an active orthosis used in back-assisted mobilization

M. Ballesteros-Escamilla¹ · D. Cruz-Ortiz¹ · I. Salgado² · I. Chairez¹

Received: 4 June 2018 / Accepted: 3 May 2019 / Published online: 17 June 2019
© International Federation for Medical and Biological Engineering 2019

Abstract

This article shows the design of a robust second-order sliding mode controller to solve the trajectory tracking problem of an active orthosis for assisting back physiotherapies. The orthosis was designed in agreement with morphological dimensions and its articulations distribution followed the same designing rules. The orthosis has six articulated arms attached to an articulated column. The orthosis was fully instrumented with actuators and position sensors at each articulation. The controller implemented a class of hybrid/position controller depending on the relative force exerted by the patient and the orthosis movement. The position information provided by each articulation was supplied to a distributed super-twisting differentiator to recover the corresponding angular velocity. A set of twisting controllers was implemented to regulate the position of the robot in agreement to predefined reference trajectories. Reference trajectories were obtained from a biomechanical-based analysis. The hybrid tracking control problem solved the automation of the assisted therapy to the patient, including the force feedback. The performance of the orthosis was tested with different dummy bodies with different resistance. The robust output feedback controller successfully tracked the reference trajectories despite the material of the dummy used during the testing. The orthosis was evaluated with two volunteers using a simple reference trajectory.

Keywords Back rehabilitation · Active orthosis · Distributed controller · Super-twisting differentiator · Twisting controller

1 Introduction

A spinal cord injury (SCI) is a damage or trauma which consequences are impairments in bowel and bladder function, mobility, and autonomic functions, along with secondary conditions such as pressure ulcers and pain [1, 2].

In addition, back disorders (BD) produced by problems with the vertebrae, joints, or discs can all cause several backache [3]. Depending on the degree of illness severity, the SCI and other BD are treated by therapy or even with a surgery that demands long periods of rehabilitation [2]. Usually, such rehabilitation process consists of physiotherapy, vertebral traction, thermotherapy, electrotherapy, and the use of wearable passive orthosis [4, 5]. However, this last option only provides a permanent posture control and the complete (active part) therapy is performed by physiotherapists [6].

In the last decades, the design of robotic devices proved their efficiency as mobilization equipment with the objective of being a tool in assisted therapies [7]. Active orthosis (AO) is a class of assisting robots with the aim of helping patients to recover their mobility abilities [8, 9]. The main advantage of using AO is that they can be programmed by the physiotherapist. Indeed, AO may perform the therapy on the patient more frequently and in the patient's home. Most of the actual AO designs offer assisted rehabilitation for upper and lower limbs [10, 11]. Lower limb exoskeletons are examples of the benefits using AO devices in mobilization

✉ D. Cruz-Ortiz
cuod.cruz.ortiz@gmail.com

M. Ballesteros-Escamilla
ballesteros_mar@hotmail.com

I. Salgado
isalgador@ipn.mx

I. Chairez
ichairezo@gmail.com

¹ UPIBI-Instituto Politécnico Nacional, Mexico City, Mexico

² CIDETEC-Instituto Politécnico Nacional,
Mexico City, Mexico

therapies, which are designed as a robotic arm manipulator with 3 degrees of freedom (DoF) for each articulation.

AO devices perform therapist-designed repetitive tasks consisting of precise movements while monitoring their advances in the rehabilitation [11]. Recent studies showed the benefits of using an active orthosis as a faster rehabilitation tool which is accepted for the patient [6, 12]. The successful applications of AO contributed to the arm rehabilitation as well as assisting the lower limb mobilization. However, there are just a few devices able to perform the active therapy for rehabilitating back pain caused by either SCI or back illnesses. Nowadays, the active therapy aimed to recover back (spinal cord) movements considers the application of lower limbs-assisted active orthosis which is releasing the weight over the spinal cord. This class of assistance is popular but it is not oriented to develop the specific and controlled movements of the vertebral region. This study has proposed a different approach where the AO is strictly centered on the middle and upper sections of the spinal cord. Such a type of orthosis represents a potential contribution to the treatment of spinal cord illnesses.

Traditional control schemes based on classical proportional derivative (PD) or proportional-integral-derivative (PID) controllers [13, 14] and computed torque control [15, 16] have been successfully implemented in many AO. However, these controllers need partial knowledge of the robot dynamics, as well as complete access to the state vector [17]. If the available measurements are the position of each joint of the orthosis, a differentiator or an observer must be implemented. Classical examples are low-pass filters, Euler-based differentiators, robust observers, or sliding mode differentiators [9, 15, 18, 19, 19, 20]. Moreover, as the AO devices are in contact with the patient, any parametric uncertainty and perturbation should be rejected to avoid any damage in the user, as well as the physical human-robot interaction (pHRI) produced by an opposite force induced by the patient into the robot. This action is commonly named an impedance control [21]. Impedance control designs can gently force the human to a desired equilibrium while limiting the applied forces on the human body.

The design of an AO requires the solution of three relevant issues that conform the main contributions issued in this manuscript: (1) the controller regulating the movement of the AO according to anatomical constraints; (2) the reference trajectories defining the accurate application of an automated therapy proposed by a medical specialist; and (3) pHRI based on impedance control designs which gently forces the robotic orthosis to move the human body to a desired equilibrium.

The introduction of impedance in the control design may limit the applied forces on the human body by the robotic orthosis [22]. These problems can be tackled with a robust controller. Sliding mode (SM) controllers and

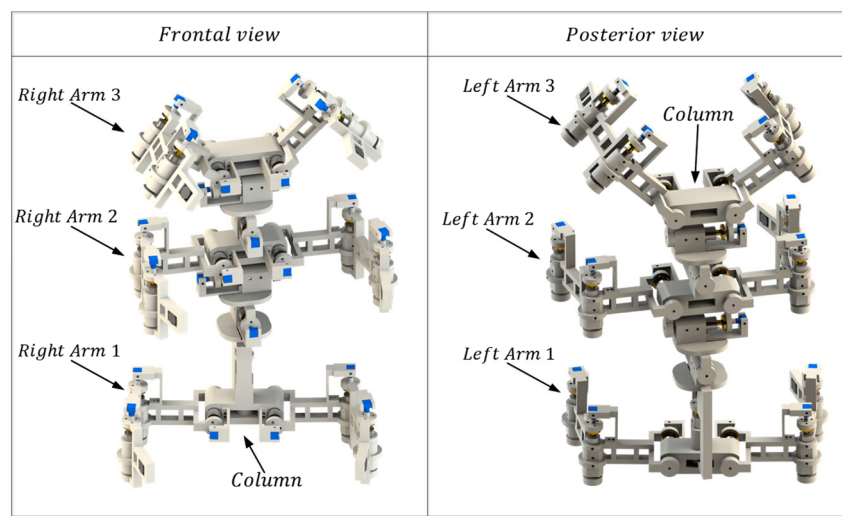
their variations have shown to be robust with respect to parametric uncertainties, presence of external perturbations, and high degree of vagueness on the mathematical model of the system to be controlled or estimated (parameters or/and states) [23, 24]. The main drawback of SM is the characteristic high-frequency oscillations that constrain the application of such controllers due to the mechanical and electronic stresses produced on actual systems. Nowadays, high-order sliding mode (HOSM) has been used for reducing such undesired behavior [25]. The twisting algorithm (TA) and the super-twisting algorithm (STA) are examples of HOSM algorithms. TA and STA serve as state feedback controllers [26, 27]. However, such algorithms can be adapted for estimating the unmeasured variables in dynamic systems, hence working as state observers [18–20].

This study presents an AO designed with 23 fully actuated DoF. Each articulation in the AO system was controlled based only on the reference trajectories provided by the physiotherapist. A regular strategy for designing reference trajectories is based on the so-called Bezier polynomials [28, 29] that are smooth and they have zero derivatives in their extreme sections. However, they demand the estimation of many parameters for designing each polynomial. Instead, this manuscript presents a different strategy based on sigmoidal functions [30]. To enforce the tracking trajectory problem, a hybrid controller is implemented with a twisting controller supplied with the velocity estimation of each link by a distributed STA working as a robust exact differentiator [2, 24]. The designed controller ensures a soft interaction between the patient and the AO. Based on the suggested AO design and the renamed AO design requirements, the contributions of this manuscript can be summarized as follows:

1. The design of a hybrid position/force robust second-order sliding mode controller to solve the trajectory tracking problem of an active orthosis for assisting back physiotherapies.
2. The designed orthosis agrees with regular morphological dimensions and articulation distribution obeying the movement capacities of the human back.
3. A set of twisting controllers regulating the position of the robot in agreement to predefined reference trajectories, but taking into account the patient's resistance.
4. The movement performance of the orthosis was tested with different dummy bodies showing different resistance against the forced movement by the orthosis.
5. The orthosis was evaluated with two volunteers using a simple reference trajectory.

The remainder of the article is organized as follows. A brief description regarding the AO mathematical model, its mechanical design, and the control proposal is presented in Section 2 (Methods). A set of numerical simulations and experimental evaluations are presented in Section 3. Some

Fig. 1 Computer-assisted design of the AO (frontal and posterior views)



concluding remarks and future trends are given in Section 4 of this paper.

2 Methods

2.1 Mechanical design

The AO for active back-assisted therapy emulated the concept of multi-legged robots. Figure 1 shows the computer-assisted draw of the frontal and posterior views of the AO. The AO has a central multi-articulated column with six independent manipulators with three DoF each one. The dimensions of the AO obey the standard anthropomorphic measures of Mexican people (1.7-m height and 80-kg weight). The AO has fixed dimensions as Fig. 2 describes. However, the orthosis can be re-designed making it usable for people with different sizes and weights. The modification implies the inclusion of linear motion bearings in the current fixed links. Notice that this modification is not a big deal if the size adjustment is not automatized. Otherwise, both the mechanical design and electronic instrumentation complicate the automatized version that must be proposed.

Figure 3 describes how the AO should be positioned in the patient. The six arms embrace the body of the patient. The upper arms are collocated on the shoulders. The middle arms embrace the upper abdominal section and the lower arms grip the hips. Figure 4 describes the instrumentation of the AO. Each articulation of the robotic orthosis is actuated by one direct current (DC) motor and its position is measured by means of a resist position sensor. The end-effector of each arm has a pressure sensor to avoid any injury in the patient when the robotic system hold him. Once a reference pressure is measured in each of these final effectors, the controller on each articulation starts the

therapy. This part of the orthosis only works when the device is attached to the patient.

2.2 Mathematical modelling

The AO proposed in this study yields to obtain a second-order nonlinear mathematical model in the joint space that obeys [23]:

$$M(\Theta(t)) \frac{d^2\Theta(t)}{dt^2} + G(\Theta(t)) + C \left(\Theta(t), \frac{d\Theta(t)}{dt} \right) \frac{d\Theta(t)}{dt} + \psi \left(\Theta(t), \frac{d\Theta(t)}{dt}, t \right) = \tau(t) + \tau_r(t) \quad (1)$$

where $\Theta = [\theta_{11} \dots \theta_{63} \alpha_1 \alpha_2 \alpha_3 \alpha_4 \alpha_5]^\top$, $\Theta \in \mathbb{R}^{23}$ is the set of actuated joints. Figure 4 offers a graphical description of each DoF in the AO. The variables labeled θ_{ij} is the angle of j th articulation in the i th leg. The variables

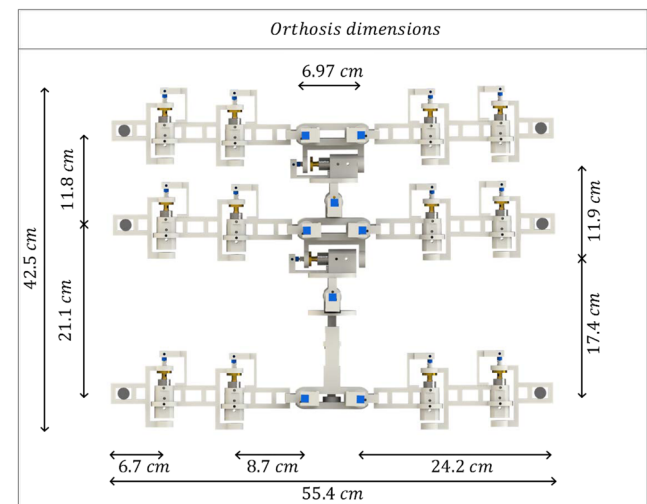
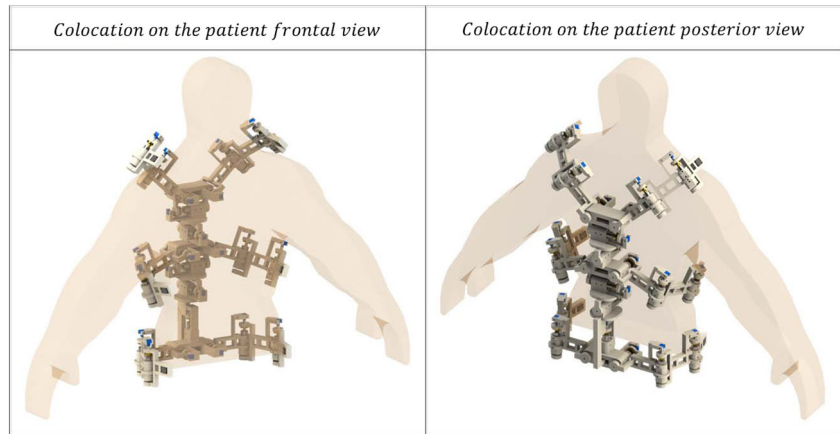


Fig. 2 General structure of the AO including the dimensions of each section in the AO

Fig. 3 Collocation of the AO over the patient. The proposed orthosis has six arms that can be mobilized independently. Their mechanical configurations allow the patient to hold by all the arms together. Even more, after the orthosis has been over-imposed on the patient's back, an elastic band can be fix at the arms tips to maintain the orthosis tightly attached to the patient

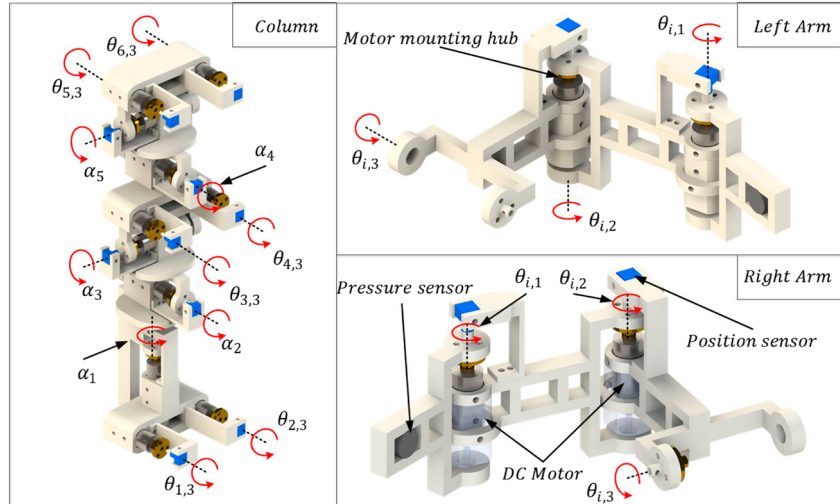


α_k represent the three angles of the articulations located at the main body of the column.

The term $\tau = [\tau_{11}, \dots, \tau_{63}, \tau_{a1}, \tau_{a2}, \tau_{a3}, \tau_{a4}, \tau_{a5}]^\top$ represents the input torque vector for the set of six fully actuated arms ($\tau_{11}, \dots, \tau_{63}$) and the column ($\tau_{a1}, \tau_{a2}, \tau_{a3}, \tau_{a4}, \tau_{a5}$). Each term τ_{ij} represents the torque for the i th arm and the j th articulation. The torques $\tau_{a1}, \tau_{a2}, \tau_{a3}, \tau_{a4}, \tau_{a5}$ correspond to the articulations included in the main body of the orthosis. The matrix M stands for the generalized inertia term, $G(\Theta)$ describes the gravitational effect terms, and $C(\Theta, \dot{\Theta})$ is the so-called Coriolis matrix. The function ψ contains all the perturbations and uncertainties affecting the model of the AO. A set of simulations was evaluated using the same reference trajectories that were evaluated on the real orthosis. Then, a developed cyber-physical model of the orthosis was used to evaluate both the proposed controller and the reference trajectories. This strategy helped to define the gains implemented in the experimental evaluation of the controller.

The term τ_r represents the effect of the constraint force induced by the patient that can oppose the orthosis movement. This opposition may come from own pathology characteristics or the therapy evolution. Usually, this force satisfies the following model $\tau_r(t) = J(\Theta(t))^\top f_{\text{ext}}$ where $J(\Theta(t))$ is the Jacobian value that relates the terminal velocity of all arms in the orthosis with the time derivative of generalized coordinates Θ , that is, if $r \in \mathbb{R}^{23}$ and $\frac{d}{dt}r \in \mathbb{R}^{23}$ are the position and the velocity of the orthosis end effectors (lateral arms), and f_{ext} is the external force associated to the patient resistance [31]. This resistance establishes the stiffness between the patient and the orthosis. Notice that f_{ext} is the resistance function of the patient against the application of the induced movement by the orthosis. The patient opposition may come from the own pathology characteristics or the therapy evolution. The physicians may establish the sequence of movements r to be executed by the orthosis.

Fig. 4 Articulated movements of the AO that describes the DoF of the whole robotic system



Then, it is necessary to consider the following position and kinematic constraints in order to define the articulations displacements which must be tracked:

$$\psi = \Phi(\Theta) \quad \frac{d\psi(t)}{dt} = J(\Theta(t)) \frac{d\Theta(t)}{dt} \quad J(\Theta(t)) = \frac{d\Phi(\Theta(t))}{d\Theta} \quad (2)$$

Based on the relationship between the end effector position and the generalized coordinates Θ , the orthosis dynamics expressed in the operation space satisfies:

$$M_r(\psi(t)) \frac{d^2\psi(t)}{dt^2} + C_r \left(\psi(t), \frac{d\psi(t)}{dt} \right) \frac{d\psi(t)}{dt} + G_r(\psi(t)) + \Phi_r \left(\psi(t), \frac{d\psi(t)}{dt}, t \right) = J^{-\top}(\psi(t)) \tau(t) + f_{\text{ext}}(t) \quad (3)$$

where

$$\begin{aligned} M_r(\psi) &= J^{-\top}(\psi) M(\psi) J^{-1}(\psi) \\ C_r \left(\psi, \frac{d\psi}{dt} \right) &= J^{-\top}(\psi) \left(M(\psi) \frac{dJ^{-1}(\Theta)}{dt} + C \left(\psi, \frac{d\psi}{dt} \right) J^{-1}(\psi) \right) \\ G_r(\psi) &= J^{-\top}(\psi) G(\psi) \\ \Phi_r \left(\psi, \frac{d\psi}{dt}, t \right) &= J^{-\top}(\psi) \psi \left(\psi, \frac{d\psi}{dt}, t \right) \end{aligned}$$

The matrix M_r has a well-defined inverse matrix. A robust solution for the force control required introducing the position coordinates and the operation space states defining the patient resistance which could be modeled as $f_{\text{ext}} = K_{st}(\phi_s - \phi)$. Here $\phi_s \in \mathbb{R}^{23}$ represents the position where the distal elements of the orthosis should move back if the external force disappears. The term $K_{st} \in \mathbb{R}^{23 \times 23}$ is a symmetric and positive definite matrix that describes the environment stiffness. The identification of the matrix K_{st} can be obtained with the application of a parametric identification algorithm. The solution of this problem can be obtained with additional electronic instrumentation. Some charge cells (multi-directional) must be inserted at each articulation to determine the relationship between the forces and the tracking errors. Then, the matrix version of the least mean square approach yields to the estimated value of K_{st} . However, such modeling oversimplifies the patient resistance to the orthosis movements.

The robust solution may produce control actions with high-amplitude oscillations. An adaptive approach of the impedance control requires an additional part. If an external force acts on the set of end effectors (like the resistance enforced by the patient), the objective of the adaptive impedance controller is to cause the end effector to respond according to some defined dynamics. This part of the controller allows to change the dynamic response of the orthosis with respect to the patient. For example, if the

patient should not be forced by the orthosis, the desired dynamics can only track the patient movements and then, to reduce the impedance response to zero in the best case [22, 32, 33]. On the contrary, if the orthosis must force the patient to complete a specific therapy, the desired dynamics can be adjusted to keep the resistance in an acceptable range. The bounds of this range should be proposed by a medical doctor. Usually, the impedance control is proposed in terms of a reference motion trajectory and the desired dynamic relationship between the position error and the interaction force f_{ext} . Impedance control has no objective of tracking motion and force, but rather to control motion and force simultaneously to develop a predefined relationship between the interaction forces and the orthosis position, that is, the mechanical impedance:

$$M_m \frac{d^2\Delta(t)}{dt^2} + C_m \frac{d\Delta(t)}{dt} + K_m \Delta(t) = f_{\text{ext}} \quad (4)$$

$$\Delta = \psi_d - \psi$$

In Eq. 4, ψ_d is determined by Eq. 3 that corresponds to the commanded ending effector position in the workspace which is defined by the orthosis movement. The variable ψ_d corresponds to the desired responses to the external force characterized by the commanded position. For example, if the therapy demands that the orthosis should not enforce any resistance to the patient movements, then ψ_d must correspond to the relative movements executed by the patient's body at the positions on the back where the end effects are placed.

This condition implies the necessity of designing ψ_d once the matrices M_m , C_m as well as the vector K_m are given positive definite matrices which specify the desired dynamic relationship between the reference position error Δ and the interaction force f_{ext} . This part of the problem is commonly known as trajectory planning which is a subject that has been deeply explored by several authors.

The design of M_r , C_r as well as the vector G_r is a challenging problem in the case of a multi-articulated device such as the proposed orthosis. Then, it is not expected that the treating physician should design such parameters. What the physician could do is to establish the maximum allowed force between the orthosis and the patient. Based on this information, the designer could adjust M_r , C_r as well as the vector G_r to fulfill such restrictions. The design procedure is the following:

Notice that Δ can be estimated on-line and together the proposed external force f_{ext} defines the relationship for $M_m \in \mathbb{R}^{23 \times 23}$, $C_m \in \mathbb{R}^{23 \times 23}$, and $K_m \in \mathbb{R}^{23 \times 23}$. Usually, these matrices are constant diagonals and can be calculated on-line based on the forgetting-factor matrix identification method:

$$[M_m \ C_m \ K_m] = \int_{\tau=0}^t e^{-\lambda(t-\tau)} \left(\Gamma(\tau) \Gamma^\top(\tau) \right)^{-1} \left(f_{\text{ext}}(\tau) \Gamma^\top(\tau) \right) d\tau \quad (5)$$

The matrix estimation algorithm can be solved on-line or off-line (using the data obtained during the preliminary testings of the AO). Notice that the controller proposal given in this study does not consider the regular method used in impedance control theory. Usually, the desired impedance can be attained by using impedance control to change dynamics of the orthosis but in this case, the expected solution must offer a different solution, as it has been explained earlier. The variations of patient movement force to calculate M_m , C_m , and K_m on-line to satisfy the trajectories generated by the patient. Besides, the inclusion of f_{ext} in the desired force dynamics decouples the control design in two diversified problems, position and force that can act simultaneously.

The substitution of f_{ext} calculated in Eq. 4 in Eq. 3 yields to:

$$(M_r(\psi(t)) + M_m) \frac{d^2\psi(t)}{dt^2} + \left(C_r \left(\psi(t), \frac{d\psi(t)}{dt} \right) + C_m \right) \frac{d\psi(t)}{dt} + G_r(\psi(t)) + K_m \psi(t) + \Phi_r \left(\psi(t), \frac{d\psi(t)}{dt}, t \right) = J^{-\top}(\psi(t)) \tau(t) + \Pi(t) \quad (6)$$

$$\text{where } \Pi(t) = M_m \frac{d^2\psi_d(t)}{dt^2} + C_m \frac{d\psi_d(t)}{dt} + K_m \psi_d(t).$$

2.3 The hybrid orthosis control problem

The control design for the AO obeys a mixed structure. The first part of the control design must enforce the tracking of a reference trajectory that corresponds to the planned therapy. The second section of the controller avoids injuring the patient because the tracking robust position control for AO may produce strong control forces on the human body [34, 35].

The solved tracking control challenge was to provide the finite-time convergence between the articulation positions and the reference (desired) trajectories despite the presence of uncertainties forced by the interaction between the orthosis and the patient. Notice that this orthosis is not useful for patients who have deficiencies in the autonomous control of the lumbar spine. Indeed, the device only executes the programmed movements that evidently include keeping the patient immobilized. The reference trajectory was provided by a predefined flow of desired articular positions $\Theta^* = [\theta_{11}^* \theta_{12}^* \dots \theta_{62}^* \theta_{63}^* \alpha_1^* \alpha_2^* \alpha_3^* \alpha_4^* \alpha_5^*]$ that were suggested to fulfill the automatic physiotherapy. Notice that $\psi^* = \Phi(\Theta^*)$ exists. The trajectories of these reference angles were obtained by a biomechanical study associated to the standard physiotherapy method used in the treatment of back injuries and/or illnesses [2].

Usually, physiotherapy procedures include the repeated application of small forces to induce controlled movements of the vertebra. These movements obey some rules that

provoke non-inflammatory processes and are aimed to recover mobility and decompression between muscles and vertebrae [5]. Clearly, these movements must be completed in a predefined time window. This period of time is defined by the physiotherapist. Therefore, finite-time convergence is required considering that reference trajectories must be tracked before the end of the corresponding time window. Formally, the control design must solve the following problem

$$\|\Theta(t) - \Theta^*(t)\| = 0, \quad \forall t \geq T_c$$

or equivalently $\|\psi(t) - \psi^*(t)\| = 0$. In the previous equation, the time T_c corresponds to the moment when each single movement must be completed by the orthosis. This time is defined by the time window proposed in each treatment strategy. So the control must ensure the convergence to the reference trajectory at a finite-time less than all the feasible T_c . Moreover, the feasible control design must consider that just the position can be used, but no velocity data are available.

Finite-time is a remarkable characteristic of sliding mode controllers and observers. Even more, they are able to solve the tracking trajectory despite the presence of modeling uncertainties and external perturbations. These two characteristics appear as major contributions from the theoretical point of view. In this sense, the execution of a proposed therapy must be finished in a given period of time. Therefore, both theoretical aspects should match and this is the reason justifying the application of sliding mode algorithms. On the other hand, the actual implementation of sliding mode algorithms implies the presence of sampling frequency, actuator imperfections, limited bandwidth, etc, which are not allowing the practical realization of the finite-time convergence. However, the rest of the relevant sliding mode characteristics such as robustness against parametric uncertainties and non-modeled dynamics are preserved. This fact justifies the implementation of the controller proposed in this study. Nevertheless, we believe that at least, the theoretical section must be well justified in the terms described here.

The controller must consider not forcing the patient movement beyond a safety operation condition, which is defined by the expert physician. The safe zone is defined by the maximum force, which is considered admissible between the patient and the orthosis. This value can be set to zero if the orthosis must not force the patient movement at any time. However, there is the option that the admissible force could be set in order to force the patient's back movement, but if the patient offers resistance, leading to a given responsive force F_r . Then, the controller must use the section devoted to keep the relative force between the orthosis and the patient in the given admissible region $F_{\text{ext}}^+ > 0$, $\|F_{\text{ext}}\| \leq F_{\text{ext}}^+$, yielding to consider that the

controller aimed to force the tracking error to zero, must not be considered.

The AO mathematical model (6) (corresponding to the trajectory tracking problem) belongs to a class of coupled second-order nonlinear systems with uncertain structures. Based on the state variable theory, the model (6) can be represented as follows:

$$\begin{aligned} \frac{d}{dt}x_a(t) &= x_b(t) \\ \frac{d}{dt}x_b(t) &= f(x(t)) + g(x_a(t))u(t) + \xi(x(t), t) \end{aligned} \quad (7)$$

where $x = [x_a^\top, x_b^\top]^\top$, $x \in \mathbb{R}^{46}$, and $x_a \in \mathbb{R}^{23}$, $x_b \in \mathbb{R}^{23}$ are the state variables of the AO (positions and velocities) proposed in Eq. 6. The vector field $f : \mathbb{R}^{46} \times \mathbb{R}^{23} \rightarrow \mathbb{R}^{23}$ collects all the known sections of Eq. 6. The function $g : \mathbb{R}^{23} \rightarrow \mathbb{R}^{23 \times 23}$ defines the input-associated function. The function $\xi : \mathbb{R}^{46} \times \mathbb{R}^+ \rightarrow \mathbb{R}^{23}$ aggregates all the uncertain sections in the model (6). The controller must be designed in such a way that the $\psi(t) - \psi^*(t)$ has a finite-time stable equilibrium point at the origin with enough robustness with respect to ξ . The system (7) has the initial condition given by $x(0) = x_0$, $\|x_0\| < \infty$. This dynamic system is a hybrid structure having two elements, the tracking and the force (impedance) controllers.

The control action $u \in \mathbb{R}^{23}$ corresponds to the torque variable τ and belongs to the following admissible set

$$U_{\text{adm}} = \left\{ u : \|u\|^2 \leq u_0 + u_1 \|x\|^2, \quad u_0, u_1 \in \mathbb{R}^+ \right\} \quad (8)$$

As we need to estimate the velocity of each joint in the AO, we need to ensure the function of the super twisting algorithm in the presence of any control action. Notice that, if $u_0 \neq 0$ and $u_1 = 0$, we arrive to a bound that characterizes any control signal obtained by the sliding mode theory, like the twisting controller. In the case of $u_0 = 0$ and $u_1 \neq 0$, we obtain a classical bound for a feedback controller. If $u_0 \neq 0$ and $u_1 \neq 0$, we obtain a mixed controller.

The previous definition in Eq. 8 is needed to ensure the uniqueness and existence of the solution for the ordinary differential equation (7). This class of controllers considers a large class of feasible algorithms including continuous and discontinuous versions. Both functions f and g were obtained directly by the application of the Euler-Lagrange method. Evidently, x_a can be clearly measured on-line by the instrumented sensors attached to the articulations of the orthosis. The function g fulfills the following constraint

$$0 < g^- \leq \|g(\cdot)\| \leq g^+ \quad g^-, g^+ \in \mathbb{R}^+ \quad (9)$$

The uncertainties ξ can represent parameters variations, external perturbations, modeling errors, etc. In this study,

by assumption, the set of perturbations $\xi(x, t)$ satisfies the following inequality [36]:

$$\begin{aligned} \|\xi(x, t)\|_{\Lambda_\xi}^2 &\leq \gamma_0 + \gamma_1 \|x\|^2 \\ \gamma_0, \gamma_1 \in \mathbb{R}^+; \quad 0 < \Lambda_\xi = \Lambda_\xi^\top &\in \mathbb{R}^{23 \times 23} \end{aligned} \quad (10)$$

The matrix Λ_ξ is proposed here to weight the contribution of each particular component of perturbation. This matrix can be determined experimentally.

This study considers the application of two well-known SM algorithms to solve the output feedback control problem described above. This proposal considers the STA as robust differentiator to recover velocity information using only the position measurements. Once the tracking error is obtained, the STA obtains the derivative of it without any velocity measurement. The controller scheme is proposed in a decentralized manner in order to simplify the solution of the tracking problem, that is:

The system given in Eq. 7, can be represented as the composition of the following second-order single-input single-output systems

$$\begin{aligned} \frac{d}{dt}x_{a,i}(t) &= x_{b,i}(t) \\ \frac{d}{dt}x_{b,i}(t) &= f_i(x(t)) + g_i(x_a(t))u_i(t) + \xi_i(x(t), t) + \eta_i(x_a(t), u(t)) \end{aligned}$$

The product of elements $g_{i,j}u_j$ for $i, j = 1 : n$ and $i \neq j$ is included in $\eta_i(x_a(t), u(t))$ that is

$$\eta_i(x_a(t), u(t)) = \sum_{j=1, j \neq i}^n g_{i,j}(x_a(t))u_j(t)$$

The term $\xi_i(x, t)$ is the i th component of $\xi(x, t)$. By the arguments proposed above, the following inequality is justified:

$$|\eta_i(x_a(t), u(t))|^2 \leq g^+ (u_0 + u_1 \|x\|^2), \quad \forall t \geq 0$$

Considering the inequality (10), one may argue that

$$|\xi_i(x(t), u(t), t)| \leq \gamma_0 + \gamma_1 \|x\|^2, \quad \forall t \geq 0$$

Now, the problem formulation given above can be rephrased as follows. Given an output reference trajectory, $x_a^* \in \mathbb{R}^{23}$ for the system (7), to design a set of decentralized output feedback controllers, which regardless of the unknown non-modeled dynamics, or external disturbances, (both lumped in an additive signal η_i), forces the states x to track the desired reference trajectories, with the tracking error restricted to a small neighborhood of the origin and proportional to the level of uncertainties and perturbations. The possible sources of uncertainties are the presence of non-modeled effects (like frictions, backlash) and the presence of some external perturbations. All these phenomena motivated the application of a robust controller to solve the tracking trajectory problem. Moreover, the

class of the proposed controller forced the finite-time convergence of the actual orthosis states and the reference trajectories. The SM controller is described as

$$\begin{aligned} u_i = & k_{a,i}(x_a(t)) \operatorname{sign}(\delta_{a,i}(t)) + k_{b,i}(x_a(t)) \operatorname{sign}(\hat{\delta}_{b,i}(t)) \\ & - g_i^{-1}(x_a(t)) [f_i(x(t)) + \eta_i(x_a(t), u(t), t) - u_{i,f}] \end{aligned} \quad (11)$$

where $\delta_{a,i} = x_{a,i} - x_{a,i}^*$ is the tracking trajectory error and $\hat{\delta}_{b,i}$ is the estimation for the time derivative of $\delta_{a,i}$ that is obtained by means of the STA. The gains $k_{a,i}$ and $k_{b,i}$ were calculated in such a way that they fulfilled

$$\begin{aligned} k_{a,i} &= g_i^{-1}(x_a(t)) \bar{k}_{1,i} \\ k_{b,i} &= g_i^{-1}(x_a(t)) \bar{k}_{2,i} \end{aligned} \quad (12)$$

where $\bar{k}_{1,i}$ and $\bar{k}_{2,i}$ are negative scalars to enforce the convergence of the tracking error. The control section labeled $u_{i,f}$ is included in the design to compensate the force effect induced by the patient over the orthosis. Notice that $u_{i,f}$ is zero if the patient does not offer opposition to the orthosis.

As usual, the function $\operatorname{sign}(z)$ satisfies the following definition [23]

$$\operatorname{sign}(z) = \begin{cases} +1 & \text{if } z > 0 \\ [-1, +1] & \text{if } z = 0 \\ -1 & \text{if } z < 0 \end{cases} \quad (13)$$

If the controller proposed in Eq. 11 is applied over the dynamics of Eq. 1, the tracking error satisfies the following differential equation

$$\begin{aligned} \frac{d}{dt} \delta_{a,i}(t) &= \delta_{b,i}(t) \\ \frac{d}{dt} \delta_{b,i}(t) &= f_i(x(t)) + \xi_i(x(t), t) - h_i(x_i^*(t), t) + \\ &\quad \bar{k}_{a,i} \operatorname{sign}(\delta_{a,i}) + \bar{k}_{b,i} \operatorname{sign}(\hat{\delta}_{b,i}) + u_{i,f}(t) \end{aligned} \quad (14)$$

The design of $u_{i,f}(t)$ is presented in the following subsection. The function h_i is used to define the right-hand side of the dynamic reference system, that is

$$\begin{aligned} \frac{d}{dt} x_{a,i}^*(t) &= x_{b,i}^*(t) \\ \frac{d}{dt} x_{b,i}^*(t) &= h_i(x_i^*(t), t), \quad h_i : \mathbb{R}^2 \times \mathbb{R}^+ \rightarrow \mathbb{R} \end{aligned} \quad (15)$$

where $x_{a,i}^* \in \mathbb{R}$ corresponds to the reference angles and $x_{b,i}^* \in \mathbb{R}$ corresponds to its corresponding reference velocity. The vector $x_i^* \in \mathbb{R}^2$ is composed as $x_i^* = [x_{a,i}^* \ x_{b,i}^*]^\top$.

The estimation for the time derivative of $\delta_{a,i}$ was obtained by the following robust exact differentiator based on the STA [19]:

$$\begin{aligned} \frac{d}{dt} \hat{\delta}_{a,i}(t) &= \hat{\delta}_{b,i}(t) + l_{a,i} |\Delta_i(t)|^{1/2} \operatorname{sign}(\Delta_i(t)) \\ \frac{d}{dt} \hat{\delta}_{b,i}(t) &= f_i(x(t)) + g_i(x_a(t)) u_i(t) + \xi_i(x(t), t) - \\ &\quad h_i(x_i^*(t), t) + \eta_i(x_a(t), u(t)) + l_{b,i} \operatorname{sign}(\Delta_i(t)) \end{aligned} \quad (16)$$

where $l_{a,i}$ and $l_{b,i}$ are the gains of the robust differentiator. The term Δ_i is defined as $\Delta_{a,i} = \hat{\delta}_{a,i} - \delta_{a,i}$. A set of n differentiators were implemented to reconstruct the information of $\delta_{b,i}$.

The following extended system describes the complete dynamics of the error signal in closed-loop with the STA in Eq. 16 working as a robust exact differentiator

$$\begin{aligned} \frac{d}{dt} \delta_{a,i}(t) &= \delta_{b,i}(t) \\ \frac{d}{dt} \delta_{b,i}(t) &= \Xi_{1,i}(x(t), x^*(t), u(t), t) + \Xi_{2,i}(\hat{\delta}_{b,i}(t), \delta_{b,i}(t)) + \bar{k}_{a,i} \operatorname{sign}(\delta_{a,i}(t)) \\ \frac{d}{dt} \Delta_{a,i}(t) &= \Delta_{b,i}(t) - l_{a,i} |\Delta_{a,i}(t)|^{1/2} \operatorname{sign}(\Delta_{a,i}(t)) \\ \frac{d}{dt} \Delta_{b,i}(t) &= -l_{b,i} \operatorname{sign}(\Delta_{a,i}(t)) - \Phi_i(x(t), x^*(t), t) \end{aligned} \quad (17)$$

The terms $\Xi_{1,i}$ and $\Xi_{2,i}$ are defined as $\Xi_{1,i}(x, x^*, u, t) = f_i(x) - h_i(x_i^*, t) + \xi_i(x, t) + u_{i,f}(t)$ and $\Xi_{2,i}(\hat{\delta}_{b,i}, \delta_{b,i}) = \bar{k}_{b,i} [\operatorname{sign}(\hat{\delta}_{b,i}) - \operatorname{sign}(\delta_{b,i})]$. Additionally, the term Φ_i satisfies the following equation $\Phi_i(x(t), x^*(t), t) = f_i(x^*(t)) - f_i(x(t)) + \xi_i(x, t) + u_{i,f}(t)$.

The nature and length of movements developed by the orthosis are used to justify the existence of a positive constant Φ^+ such that the following inequality is satisfied:

$$|\Phi_i(x(t), x^*(t), t)| \leq \Phi^+ \quad \forall x \in X \subseteq \mathbb{R}^{23}, \quad \forall t \geq 0 \quad (18)$$

If the previous inequality holds, then, the result presented in [37] can be used here to prove that a positive time $T_{ST}(\Delta_{a,i}(0), \Delta_{b,i}(0))$ such that for all $t \geq T_{ST}$, $\Delta_{a,i}(t) = \Delta_{b,i}(t) = 0$ exists. This remarkable result was obtained by using a non-standard Lyapunov function $V_{ST,i}(\xi_i)$ satisfying the following structure:

$$V_{ST,i}(\xi_i) = \xi_i^\top P_{1,i} \xi_i \quad (19)$$

with $\xi_i^\top := [|\Delta_{1,i}|^{1/2} \operatorname{sign}(\Delta_{1,i}) \ \Delta_{2,i}]$. The matrix $P_{1,i} \in \mathbb{R}^{2 \times 2}$ is a positive definite and symmetric matrix.

In [24], a composite Lyapunov function was proposed to show that each extended system (17) has a robust finite-time stable equilibrium point. For the problem tackled in this paper, the previous statement means that for every admissible perturbation Ξ_i satisfying $|\Xi_i| \leq \Xi_i^+$, $\Xi_i^+ > 0$, and every bounded initial condition, a finite-time $T_i(\delta_{a,i}(0), \delta_{b,i}(0))$ so that a trajectory of system (17) starting at time $t = 0$ converges to the origin in finite-time, i.e., $[\delta_{a,i}(t), \delta_{b,i}(t)] = 0$ for $t_i > T_i$, despite of the perturbation Ξ_i exists. In this case, the function $V_{T,i}(\delta_i, \delta_{i+n})$ is given by

$$V_{T,i}(\delta_{a,i}, \delta_{b,i}) = (\pi_{1,i} |\delta_{a,i}| + 0.5 \delta_{b,i}^2)^{3/2} + \pi_{2,i} \delta_{a,i} \delta_{b,i} \quad (20)$$

The constant scalars $\pi_{1,i}$ and $\pi_{2,i}$ must be positive and satisfy $a \pi_{1,i} = p + 2\Xi_i^+ + \frac{2^{3/2}}{3}\pi_{2,i}$ with p any positive scalar.

It seems natural to consider an extended Lyapunov function satisfying the structure

$$V_i(\Delta_{a,i}, \Delta_{b,i}, \delta_{a,i}, \delta_{b,i}) = V_{ST,i}(\xi_i) + V_{T,i}(\delta_{a,i}, \delta_{b,i}) \quad (21)$$

to prove the stability of closed-loop system presented in Eq. 17. However, it is not a straightforward task to get this result based on the individual results described above.

So finally, the following storage function

$$\begin{aligned} V(\Delta_a, \Delta_b, \delta_a, \delta_b) &= \sum_{i=1}^n V_i(\Delta_{a,i}, \Delta_{b,i}, \delta_{a,i}, \delta_{b,i}) \\ \delta_a &= [\delta_{a,1}, \dots, \delta_{a,n}]^\top \quad \delta_b = [\delta_{b,1}, \dots, \delta_{b,n}]^\top \\ \Delta_a &= [\Delta_{a,1}, \dots, \Delta_{a,n}]^\top \quad \Delta_b = [\Delta_{b,1}, \dots, \Delta_{b,n}]^\top \end{aligned} \quad (22)$$

can be used to prove the existence of a robust finite-time stable equilibrium point for the entire second-order system used to represent the dynamical behavior of the back orthosis developed in this study. This function is presented here as the composition of the individual functions proposed for the twisting and STA because the forward complete property of the device used to design the orthosis.

Remark 1 The twisting controller proposed in Eq. 11 can be substituted by a linear structure

$$u_i(\delta_{a,i}, \hat{\delta}_{b,i}) = k_{a,i}\delta_{a,i} + k_{b,i}\hat{\delta}_{b,i} \quad (23)$$

The stability of the equilibrium point of the closed-loop system formed by this controller based on the estimated velocity by STA has been proved in [38]. Even when only practical stability can be proven using this controller, the high-frequency oscillations forced by the twisting controller can be attenuated. Nevertheless, in this study, the classical twisting controller without linear terms was implemented.

2.4 Trajectory planning for assisted therapy

The trajectories to be tracked by the orthosis were determined as a result of a study of usual movements applied in assisted therapy for muscle-skeletal illnesses of the spinal cord. In physiotherapy, the examiner looks for those detectable differences between normal range of movements and the patients ability to do the movement. Then, the physiotherapist tries to enforce the recovery of those movements considered as normal for healthy patients.

The range of movements attained by the patient is the result of summation of individual movements of the articulations in the entire lumbar spine. Active movements are performed with the patient standing. The active movements in assisted physiotherapy by the orthosis proposed in this study are forward flexing (40 to 60

degrees), extension (20 to 35 degrees), left and right side flexing (15 to 20 degrees), left and right rotation (3 to 18 degrees), and if necessary repetitive motion of sustained postures and combined movements.

Trajectory planning for robotic systems has been tackled with different strategies. One of the most popular was the so-called Bezier polynomials. However, calculating these polynomials in embedded systems consumes significant computing resources. This paper considers a different alternative for producing the reference trajectories. The idea was to construct the reference trajectory using sigmoid functions.

These functions can be differentiated many times and their transient trajectory from one steady state to other is smooth enough. The sigmoid function is formally defined by

$$s(t) = \frac{a}{1 + be^{(t-t_k)}} + c, \quad \forall t \in [t_k, t_{k+1}] \quad (24)$$

where the parameters a , b , and c are positive scalars.

A simple mathematical calculus yields to prove that derivative of Eq. 24 is zero when $t \rightarrow \infty$ and $t \rightarrow -\infty$. Therefore, this function satisfies the regular conditions associated to the Bezier functions [39]. Moreover, sigmoid functions simplify the construction of reference trajectories. The following procedure shows how to construct a simple example of a reference trajectory when a particular articulation must move from an initial angle ζ_0 to a final angle ζ_f in a time period of $d_t = t_{k+1} - t_k$ seconds:

- Fix the value $\frac{a}{1+b} + c = \zeta_0$
- Fix the value $\frac{a}{1+be^{d_t}} + c = \zeta_f$
- Fix the value $\frac{a}{1+be^{0.5d_t}} + c = 0.5(\zeta_f - \zeta_0)$

In the previous terms $e^{(\cdot)}$ represents the exponential function. The solution of the previous nonlinear algebraic system yields to a third-order polynomial respect to the parameter b given by

$$b^3 + w_2 b^2 + w_1 b + w_0 = 0 \quad (25)$$

where w_2 , w_1 , and w_0 can be easily calculated. According to the appendix 1 in [40], if $\Omega_1^2 - 4\Omega_0^3 \geq 0$ ($\Omega_0 = w_2^2 - 3w_1$, $\Omega_1 = 2w_2^3 - 9w_1w_2 + 27w_0$), then

$$\begin{aligned} b &= -\frac{w_2 + C_1 + C_2}{3} \\ C_1 &= \left(\frac{\Omega_1 - \sqrt{\Omega_1^2 - 4\Omega_0^3}}{2} \right)^{1/3} \quad C_2 = \left(\frac{\Omega_1 + \sqrt{\Omega_1^2 - 4\Omega_0^3}}{2} \right)^{1/3} \end{aligned} \quad (26)$$

is the real root of cubic equation (25).

Once the solution for b is gotten, the parameter a can be obtained as solution of

$$a = \frac{0.5(\zeta_f - \zeta_0)(1 + b)(1 + be^{d_t})}{b(1 - e^{d_t})} \quad (27)$$

The parameter c is given by

$$c = \zeta_0 - \frac{a}{1 + b} \quad (28)$$

Based on the structure of the sigmoid function proposed in Eq. 24, it is simple to get the reference function h_i by a simple derivation procedure $h_i(t) = \frac{ab^2}{(1+be^t)^3}$. Notice that even when the final solution of parameters is obtained by the third-order polynomial, the method presented in this study uses the natural characteristics of sigmoid functions. In order to justify the application of sigmoid functions instead of classical Bezier polynomials, the calculus of both solutions was evaluated in the same computer with equal characteristics (microprocessor, memory and operating system). Matlab® software was used to evaluate the solution of both problems. An improvement of 43 % in execution time was obtained when simulation times were compared favoring the application of sigmoid functions. This condition motivates the application of sigmoid functions instead of classical polynomials.

All the reference trajectories were proposed according to the regular movements suggested to patients that may suffer different kinds of back pain. These trajectories were analyzed in specialized publications regarding medical rehabilitation. Therefore, all the sigmoid functions used to design the reference trajectories of all articulations in the orthosis were designed simultaneously in order to ensure the synchronization problem. Moreover, the possibility of ensuring the finite-time convergence in all articulations, despite the presence of some kind of perturbations also serves as an indirect indicator of synchronicity in the application of therapy. As it is expected, the eventual application of this orthosis in actual therapies demands the design and implementation of patient's security system that may include a supervisor for the orthosis movement. Despite the importance of this external security system, this part of the problem is beyond the scope of this study.

3 Results

Figure 5 shows a block diagram clarifying the control implementation for the AO. The same scheme was implemented in both the numerical and the experimental evaluations.

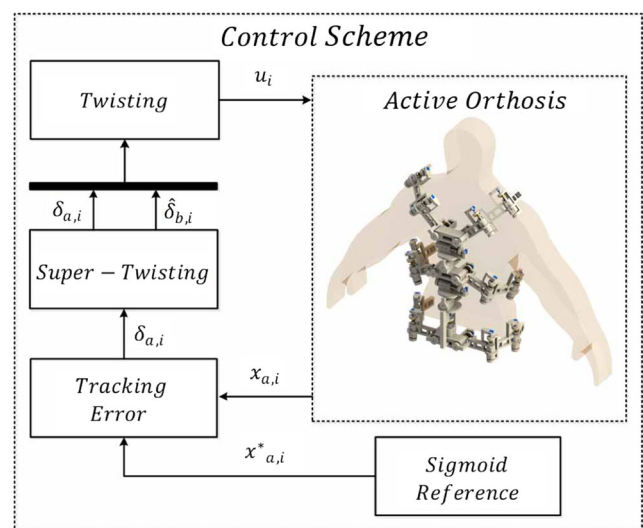


Fig. 5 Control diagram and its application on the AO

3.1 Numerical simulations

The simulation results show a virtual design of the orthosis making different movements that correspond to predefined trajectories that define a continuous therapy performed by the physiotherapist. Moreover, this section describes the performance of the robust hybrid controller described in the previous section. Figure 6 represents the AO described by simple rigid no-detailed unions. This

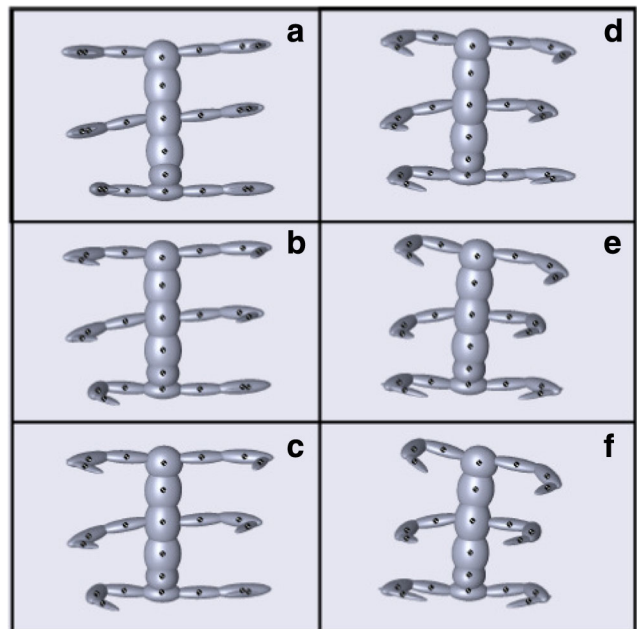
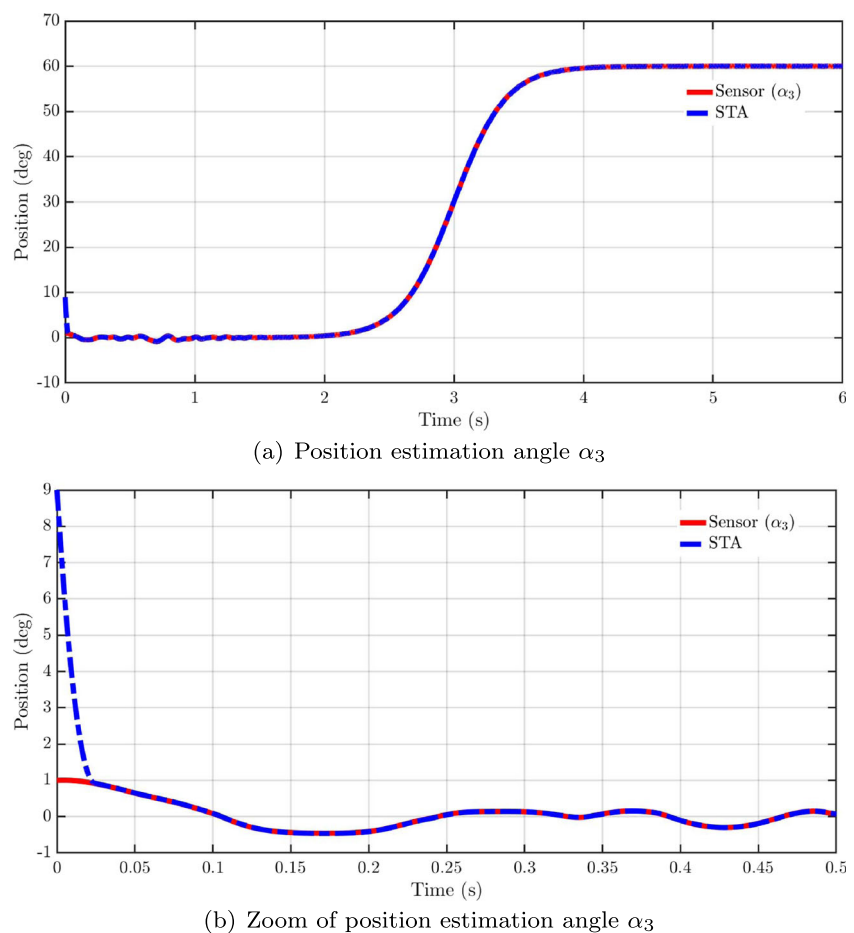


Fig. 6 a–f Movements executed by a virtual orthosis regulated by the twisting controller and STA differentiator. The simulation was numerically evaluated in Matlab using the SimMechanics Toolbox. The six different subfigures demonstrate different stages of the same therapy executed by the orthosis

Fig. 7 a, b Time evolution of a selected angle articulation and its corresponding estimation provided by the STA applied as RED



design was implemented to avoid excessive computational resources. The simulation was obtained as a solution of the numerical implementation using the SimMechanics Toolbox of Matlab. This evaluation allows to evaluate the performance of the distributed robust control based on the TA/STA scheme and the movements of the orthosis according to the specialist suggestions. Different reference trajectories were proposed to evaluate the ability of the orthosis to develop distinct therapies.

In Fig. 6, the patient appears at the first plane in front of the orthosis. The simulated model considered the actual mass and dimensions for each piece included in the AO (this condition was fixed in the model design in the computer-assisted design software). Figure 6 depicts the corresponding movements which were produced by the controller in simulation at different stages of the therapy. This figure shows six different positions of the AO where all the arms moved simultaneously accordingly to the reference trajectories. These trajectories defined the rotation of the torso from -20 to 20 degrees.

The STA working as a RED improves the tracking performance when the twisting controller is applied. This is a consequence of its robustness against uncertainties in the

model and perturbations in the output. The tracking error was obtained after the state estimation of the velocity for each joint of the robot. Figure 7a shows the reconstructed position of α_3 link localized in the column of the AO. A second graph was included with a closer view of the state estimation process where the approaching of the estimation error to the origin is confirmed. Notice that the actual and estimated velocities are indistinguishable from each other after 0.05 s (Fig. 7b). Before 0.05 s, the trajectories of the STA reach the real sensor measurements. By the invariant of the SM surface [23], once the trajectories reach the surface, they do not leave it after. Notice that this error is observed only during the transient period. After 4 s, the absolute value of this error is bounded with a maximum value of 1.0 degree/s. If we consider that the proposed orthosis is moving slowly, then we may argue that such an error will not have a relevant impact on the tracking trajectory exerting.

Figure 8 depicts the velocity estimation. The continuous red line is the analytic solution of the derivative of the sigmoidal function chosen as the reference trajectory. The dotted black line is the available measure obtained by the virtual sensor in SimMechanics toolbox [®]. Notice that the STA algorithm estimates the velocity and at the same time,

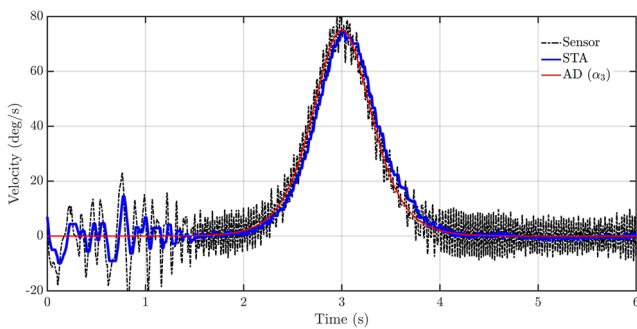


Fig. 8 Time evolution of measured angular velocity for a selected articulation and its corresponding estimation provided by the STA applied as RED. This figure also shows the comparison of the measured velocity and the analytically angular velocity calculated with the proposed sigmoid function

it rejects high-frequency oscillations. This behavior will improve the tracking performance. The velocity estimation takes less than 1 s. Once the velocity estimation is obtained with the STA, the tracking error can be easily obtained. To characterize the efficiency and accurateness of the velocity estimation by STA, the error between angular velocity measured in one single articulation and the estimated one is presented in Fig. 9. The convergence to the origin of the velocity error after just 2 s emphasizes the robustness capacity of the STA.

In order to validate the STA application as RED, a special set of simulations including noise effect on the quality of the velocity estimations was developed. Figure 10 shows the comparison of the estimated velocity if the noise is considered in the measured signal. The effect of noise affects the estimated velocity, but the velocity imprecision is not significant in terms of the application in the output-based controller.

Figure 11 depicts the simulation results for the tracking trajectory task using the TA as a robust controller. In this figure, the convergence between the reference trajectory and the real angle of the corresponding articulation evidenced the performance of the TA compared with the tracking

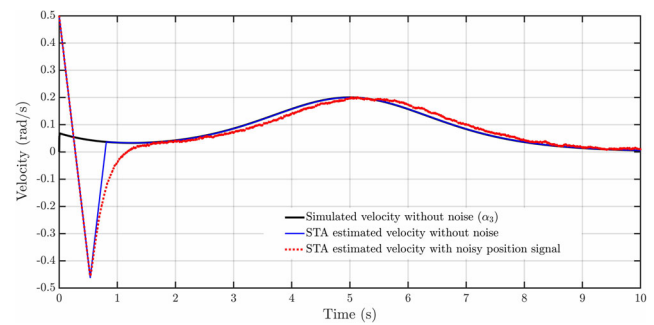


Fig. 10 Time evolution of measured angular velocity for a selected articulation and its corresponding estimation provided by the STA applied as RED. This figure demonstrates the effect of noise on the estimated velocity

result obtained with the PD controller. This convergence confirmed the better performance of the controller proposed in this study. Moreover, the fast convergence of the tracking error ensures a good performance as a wearable mobilizing device. Similar results were obtained for all the other articulations.

Figure 12 demonstrates the tracking of two articulations using the TA controller. This figure is proposed here to highlight how the proposed controller enforced the tracking of the reference trajectories with a small (less than 0.5 degrees) dithering. This dithering is a consequence of two aspects: the sampling period used in the orthosis experimental evaluation and the natural resistance exerted by the patient. Notice that the dither appears mainly on the fastest part of the transition reference curve, which is when the orthosis may have the most reactive interaction with the patient.

Figure 13 describes the Euclidean norm of the tracking error of all the articulations. This condition was obtained by the corresponding adjustment of controller gains. Despite the faster convergence provided by the TA, high-frequency oscillations also appeared in the Euclidean norm of the tracking error. However, this condition was expected considering the discontinuous nature of Eq. 11.

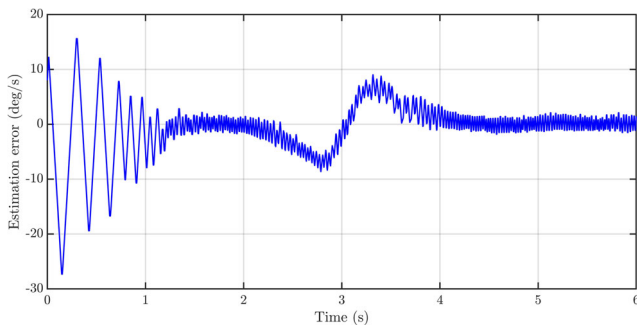


Fig. 9 Time evolution of the error obtained between measured angular velocity for a selected articulation and its corresponding estimation provided by the STA applied as RED

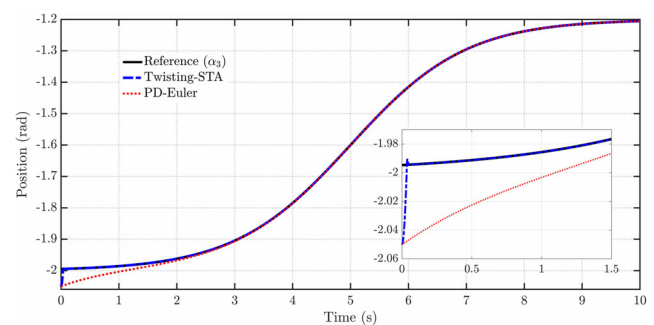


Fig. 11 Time evolution of the reference angular velocity for the selected articulation α_3 and its corresponding trajectory enforced by the TA and the PD

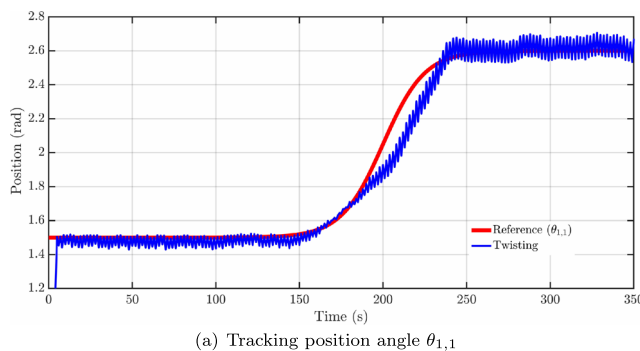


Fig. 12 a, b Time evolution of a selected angle articulation and its corresponding reference trajectory generated by the reference model

Nonetheless, the amplitude of these oscillations never grows up beyond 0.2 degrees. This condition can be observed in simulations but they were not distinguished in the actual orthosis.

The control signal enforcing the convergence of the tracking error of the angle α_3 is shown in Fig. 15. Notice that the signal presented in the aforementioned figure is the pulse width modulation (PWM) of the response calculated by the TA. If the signal seems to be aggressive, the PWM acts as a low-pass filter. The low-pass-filtered signal appears also in this figure.

The vibrations in the control signal may appear in the orthosis-patient interaction forces due to the discontinuous torque generated by the twisting controller. Although this

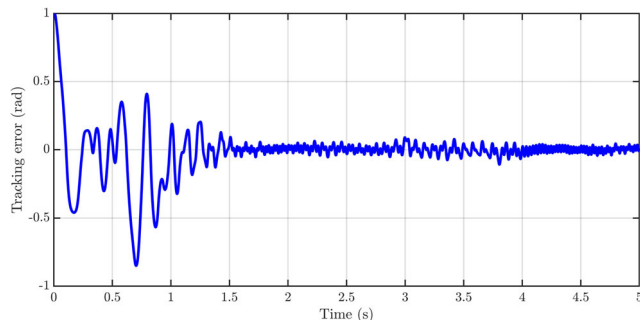


Fig. 13 Averaged time evolution of the tracking trajectory errors of all the articulations that conform the AO

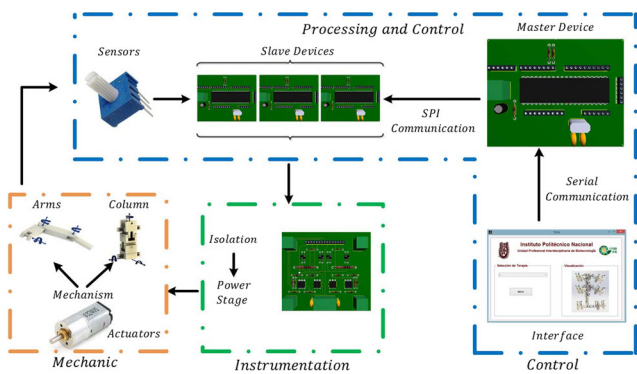


Fig. 14 Software/hardware implementation. Rotary potentiometers were used to measure the angle position in each DC motor actuates each articulation. The distributed electronic system regulates the orthosis by means of a hierarchical structure based on one master device and seven slave devices

aspect may seem a serious issue in the present application, the accurate gain tuning as well as the force compensation reduced the oscillations on the tracking trajectory as demonstrated in this study.

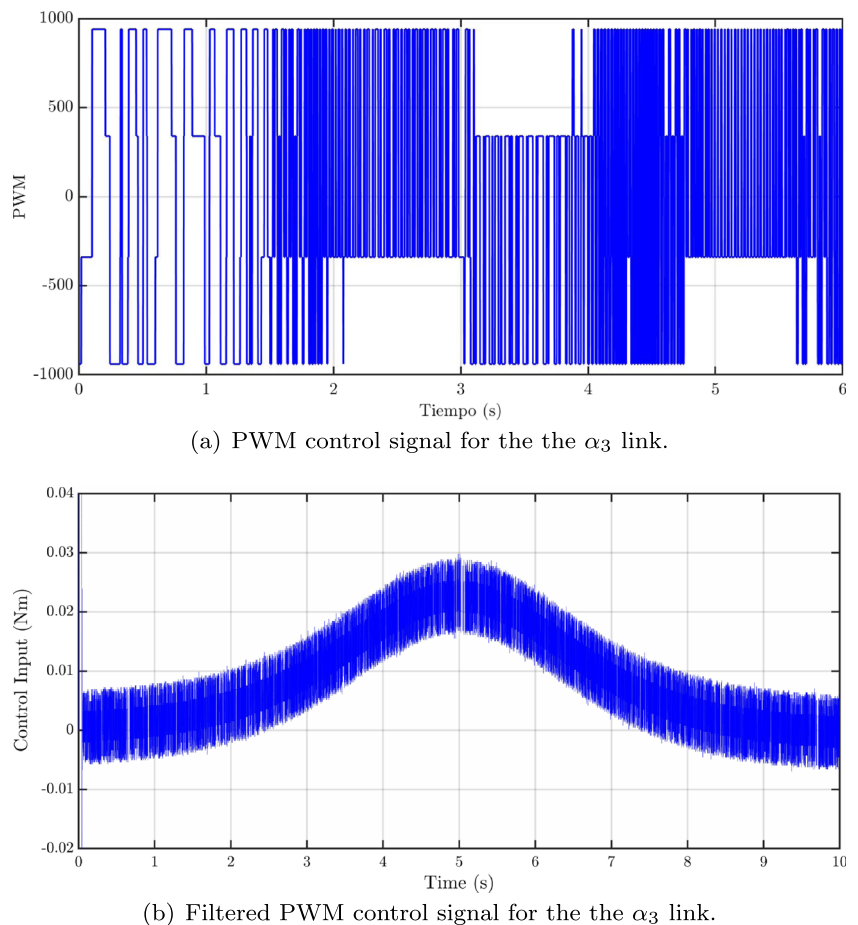
3.2 Experimental results

The instrumentation includes rotatory sensors in each DoF as well as DC motors as actuators. Notice that the angular measurements could be obtained by accurate encoders, but these may be very expensive (especially if their size must be small enough to be used in the proposed orthosis), which is not a trivial issue if the proposed orthosis is aimed to be as cheap as possible, while keeping the accurate tracking of the reference trajectories. Figure 14 describes the complete process for controlling the designed AO. This fact motivated the inclusion of rotatory variable resistors as feasible angular displacement sensors. In addition, both active analog and digital low-pass filters (with the cutting frequency of 25 Hz) were proposed to reduce the measurement noise effect. This aspect is still a matter of researching, which is beyond the scope of this study.

The sliding mode control variation is a consequence of its discontinuous structure. Nevertheless, notice that the reference trajectories are tracked with acceptable quality (in terms of both the numerical and the experimental evaluations). However, it is true that controller instrumentation with constant gains may produce transient fast movements and sometimes relevant energy consumption (Fig. 15). A reasonable solution is implementing tracking error-dependent gains which can reduce both the chattering amplitude and energy consumption. However, the experimental implementation of such adaptive laws may introduce additional complexity which must be evaluated in detail.

The power section and the digital controlled section were isolated by a set of opto-electronic devices. The

Fig. 15 **a, b** Control signal injected to the actuator corresponding to the α_3 angle



opto-isolator used was the 4N25 with range of admitted frequencies. The electronic design contemplates a set of eight microcontrollers to actuate separately each arm as well as the column. The microcontroller used in the experiment was the PIC18F4550. A master device

supervises the functionality of each slave device by serial protocol interface (SPI) communication. A graphical user interface allows the medical specialists and physiotherapists to operate the AO. A set of 23 independent controllers were placed the embedded systems. The implementation of the STA and TA followed a classical Euler discretization [41]. The discrete version of the STA with a defined sample time becomes

$$\begin{aligned} \hat{\delta}_{a,i}((k+1)T) &= \hat{\delta}_{a,i}(kT) + T \hat{\delta}_{b,i}(kT) - \\ &\quad T l_{a,i} |\Delta_i(kT)|^{1/2} \text{sign}(\Delta_i(kT)) \end{aligned} \quad (29)$$

$$\hat{\delta}_{b,i}((k+1)T) = \hat{\delta}_{b,i}(kT) + T l_{b,i} \text{sign}(\Delta_i(kT))$$

The corresponding twisting controller showed in Eq. 11 is implemented as

$$u_i(kT) = k_{a,i}(x_a(kT)) \text{sign}(\delta_{a,i}(kT)) + k_{b,i}(x_a(kT)) \text{sign}(\hat{\delta}_{b,i}(kT)) - g_i^{-1}(x_a(kT)) [\eta_i(x_a(kT), u(kT), kT) - u_{i,f}(kT)] \quad (30)$$

The microcontrollers allow to adjust T to 0.01 s in both computer and microcontroller.

Figure 16 shows different positions that can be attained by the actual orthosis. The positions obtained demonstrated

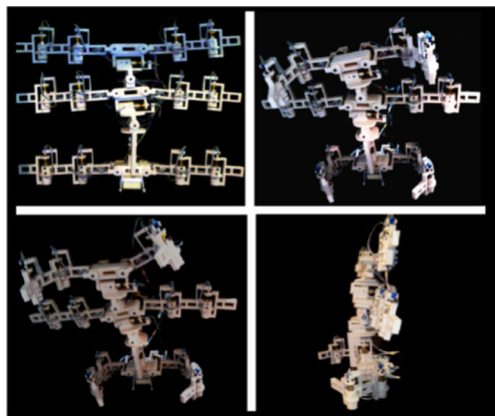


Fig. 16 Set of photographs depicting different movements of the AO. These movements correspond to specific reference trajectories proposed by the specialist

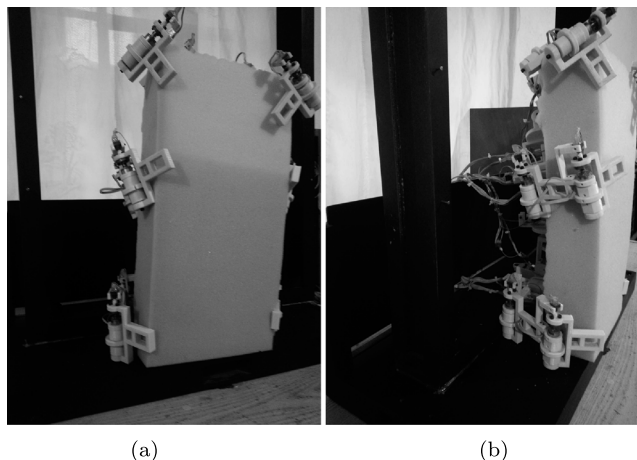


Fig. 17 a, b AO attached to the polyurethane dummy. This experiment was proposed to evaluate the controller effectiveness under the presence of some perturbations such as the resistance of the dummy material

the controller capacity to solve the trajectory-tracking problem.

A set of tests of the AO was executed on two volunteer subjects. These subjects did not have a diagnosed back illness. These subjects were informed about the objective of the experiment by an information statement. The experiments consisted on using the orthosis proposed in this study to apply diverse movements on the subjects back. The expert opinion of orthopedists from a local Hospital in Mexico city (Hospital General La Villa) served to define the reasonable movements of the AO as well the limits for the force that can be opposed by the patient.

Several tests evaluated the performance of the AO before its use in a patient. The first test consists to evaluate OA movements consisted of using soft polyurethane dummies that served to represent the patient's back. This experiment was proposed to characterize the robustness capacity of the implemented automatic controller working on the AO.

The controller was evaluated with different dummies made of polyurethane. Three different densities of the same material were used as testing elements. Despite the type of dummy, the controller succeed to track different reference trajectories (Fig. 17a for frontal view and b for the rear view). This figure demonstrates different positions of the same trajectory. These photographs are depicted to emphasize the real movement of all articulations.

A second round of experiments was executed on volunteer patients. These patients were informed regarding the objective of the study and they agreed to participate in the tests. These tests were proposed to move the volunteers' back according to the suggestions provided by a physiotherapy suggestion (Fig. 18).

The trajectories of the states in the column were monitored by the microcontrollers by a modified software that sent the actual articulation angles by a RS-232 protocol. The deviation between the reference trajectories and the ones obtained in real device was evaluated. The following mean square error measure was used to obtain a quality indicator of the orthosis performance.

$$\text{MSE}(kT) = \sum_{j=1}^M (\delta_{a,j}^2(kT) + \delta_{b,j}^2(kT)) \quad (31)$$

where M is the total number of articulations included in the robot (23 in all cases). A set of N measurements was executed during the experiment for each patient. The value of N was 50 for the first volunteer and 20 for the second volunteer using the same reference trajectory.

The values of mean square error (MSE) were similar to the ones observed during simulation processes. However, the convergence to an acceptable region defined by 0.25 degrees was attained after 20 s which is 10 times bigger than that obtained in numerical simulations. This difference depended on two factors, the limited voltage that can be applied on each DC motor used in the AO and the sampling time considered for evaluating both the differentiator and the controller. These two characteristics influenced the convergence time as notices in Fig. 19.

Fig. 18 **a, b** Different views of the volunteer using the prototype of AO in two different positions proposed as part of the therapy suggested by the physiotherapy specialist

Orthosis Implementation on a Real Patient		Orthosis Therapies	
Back View	Side View	Left Inclination	Right Inclination
			
(a) Orthosis fixed in a patient		(b) Orthosis therapy in a patient	

Fig. 19 **a, b** Time evolution of tracking trajectory between measured angle for two selected articulations under the action of the twisting controller implemented in a selected embedded device

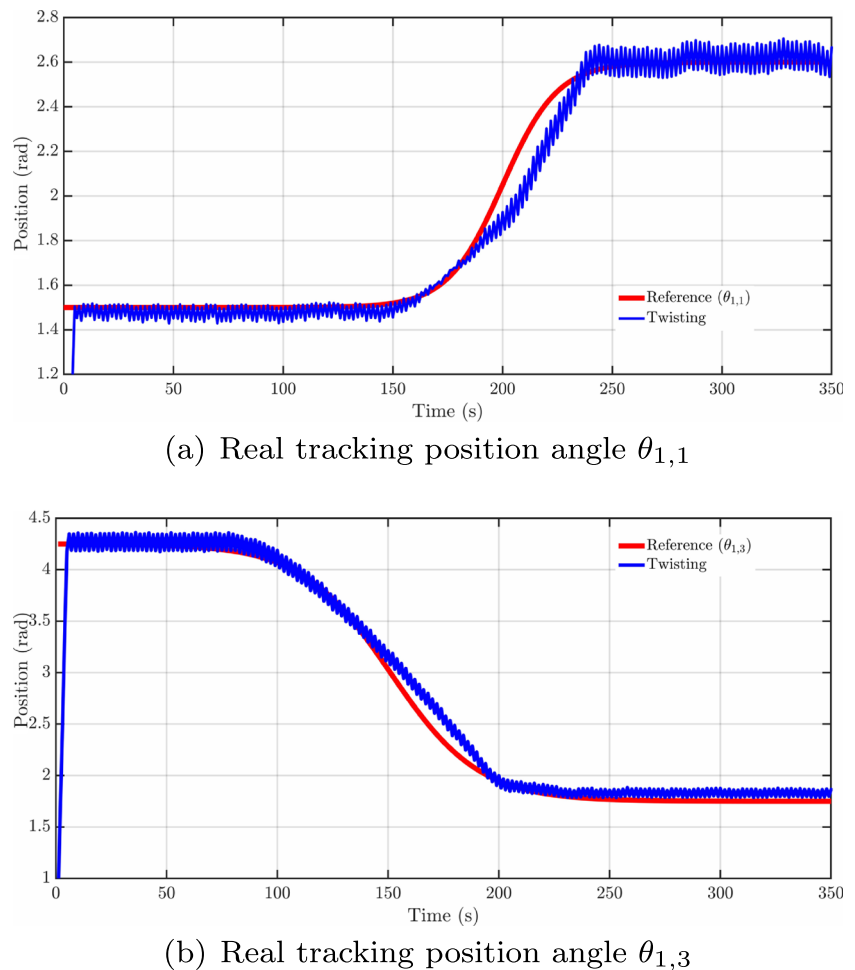


Figure 19 shows the tracking trajectory evolution of each articulation $\theta_{1,1}$ and $\theta_{1,3}$ to the desired reference paths for a particular physiotherapy. Figure 20 depicts the MSE of the experimental evaluation for a volunteer. Similar results were observed for other volunteers despite their physical characteristics, that means, weight and height. Notice that the error never grows beyond 0.4 degrees and approaches the origin within the first 20.0 s of the proposed treatment.

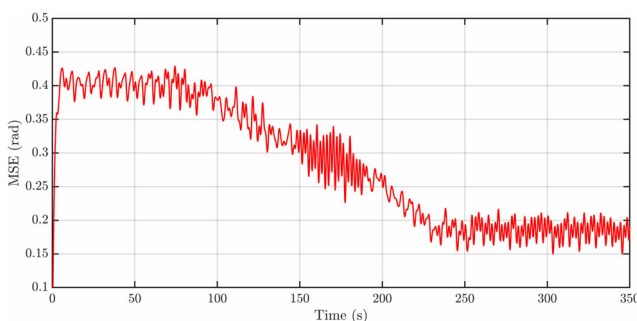


Fig. 20 The experimental MSE of the robotic orthosis

4 Conclusions

This paper describes the entire design of an AO to assist the rehabilitation of spinal cord and/or back illnesses. This device was supplied with some electromechanical sensors which were used by a robust output feedback controller. This information produces a mixed structure based on robust observation and output feedback controller which served to adjust the movement of the active orthosis. The robust observation was executed by the implementation of a decentralized RED based on the STA. Information generated by the differentiator was injected into a set of twisting controllers. All the controllers and differentiators were tested and adjusted in numerical simulations.

A basic construction of the orthosis system was used to generate some actual evaluations that validated the theoretical results achieved in this study. An instrumentation platform was implemented to execute the controllers in digital systems that were connected to a set of real actuators and sensors. Tracking results obtained in the actual orthosis were very similar to the ones observed in simulations with a maximum error of 0.4 degrees and a convergence time to

a bounded region (with bound proportional to the sampling time) less than 20.0 s.

Acknowledgments The authors acknowledge Dr. Alberto Luviano (UPIITA-IPN) for his remarkable and useful comments on the results achieved in this paper.

Funding information The authors thank the financial support provided by the National Polytechnic Institute through the Research Grants labelled SIP-20 196709, SIP-20195253.

Compliance with ethical standards

Conflict of interest The authors declare that they have no conflict of interest.

References

- Bland JH, Boushey DR (1990) Anatomy and physiology of the cervical spine. *Semin Arthritis Rheum* 20:1–20
- McGil S (2007) Low back disorders: evidenced-based prevention and rehabilitation. *Human Kinetics*. [Online]. Available: <http://books.google.com.mx/books?id=j0R4-fzBwPIC>
- White AA, Panjabi MM (1978) Clinical biomechanics of the spine. Lippincott. [Online]. Available: <http://books.google.com.mx/books?id=U5NsAAAAMAAJ>
- Eisenberg MG (1995) Dictionary of rehabilitation. Springer Publishing Company
- Bergmark A (1989) Stability of the lumbar spine. *Acta Orthopædica Scandinavica* 230:1–54
- Valentin GH, Pedersen LN, Maribo T (2014) Wearing an active spinal orthosis improves back extensor strength in women with osteoporotic vertebral fractures. *Prosthetics Orthotics Int* 38(3):232–238. [Online]. Available: <https://doi.org/10.1177/0309364613497393>
- Olivier J, Ortlib A, Bouri M, Bleuler H (2015) Mechanisms for actuated assistive hip orthoses. *Robot Auton Syst* 73:59–67. wearable Robotics
- Syvert GW (1987) External spinal orthotics. *Neurosurgery* 20(4):642–649
- Luenberger L, Colombo G, Riener R, Dietz V (2004) Biofeedback in gait training with the robotic orthosis lokomat. In: IEMBS 26th Annual international conference of the IEEE engineering in medicine and biology society, vol 2, pp 4888–4891
- Hyun DJ, Park H, Ha T, Park S, Jung K (2017) Biomechanical design of an agile, electricity-powered lower-limb exoskeleton for weight-bearing assistance. *Robot Auton Syst* 95:181–195
- Asbeck AT, Schmidt K, Walsh CJ (2015) Soft exosuit for hip assistance. *Robot Autonom Syst* 73:102–110. wearable robotics
- Giovacchini F, Vannetti F, Fantozzi M, Cempini M, Cortese M, Parri A, Yan T, Lefebvre D, Vitiello N (2015) A light-weight active orthosis for hip movement assistance. *Robot Auton Syst* 73:123–134. wearable robotics
- Spong M, Hutchinson S, Vidyasagar M (2006) Robot modelling and control, F. edn. Wiley
- Kingsley C, Poursina M, Sabet S, Dabiri A (2017) Logarithmic complexity dynamics formulation for computed torque control of articulated multibody systems. *Mech Mach Theory* 116:481–500. [Online]. Available: <http://www.sciencedirect.com/science/article/pii/S0094114X1630221X>
- Castaneda A, Luviano A, Chairez I (2014) Robust trajectory tracking of a delta robot through adaptive active disturbance rejection control. *IEEE Trans Control Syst Technol*, 99. <https://doi.org/10.1109/TCST.2014.2367313>
- Codourey A (1996) Dynamic modelling and mass matrix evaluation of the delta parallel robot for axes decoupling control. In: Proceedings of the 1996 IEEE/RSJ international conference on intelligent robots and systems (IROS), pp 1211–1218
- Jankowski K, Brussel HV (1992) An approach to discrete inverse dynamics control of flexible-joint robots. *IEEE Trans Robot Autom* 8(5):651–658
- Moreno J, Sánchez T, Cruz-Zavala E (2014) Una función de lyapunov suave para el algoritmo super-twisting. In: Proceedings of the XVI LatinAmerican automatic control congress
- Levant A (1998) Robust exact differentiation via sliding mode technique. *Automatica* 34(3):379–384
- Moreno J, Alvarez J, Rocha-Cozatl E, Diaz-Salgado J (2010) Super-twisting observer-based output feedback control of a class of continuous exothermic chemical reactors. In: Proceedings of the 9th international symposium on dynamics and control of process systems (DYCOPS). Leuven, pp 727–732
- Raibert MH, Craig JJ (1981) Hybrid position/force control of manipulators. *J Dyn Syst Measur Control* 103(2):126–133
- Song P, Yu Y, Zhang X (2017) Impedance control of robots: an overview. In: 2017 2nd international conference on cybernetics, robotics and control (CRC), pp 51–55
- Utkin V, Guldner J, Shi J (2009) Sliding mode control in electro-mechanical systems, 2nd edn. Automation and Control Engineering
- Moreno J (2012) A lyapunov approach to output feedback control using second-order sliding modes. *IMA J Math Control Inf Adv*
- Pisano A, Davila A, Fridman L, Usai E (2008) Cascade control of pm dc drives via second-order sliding-mode technique. *IEEE Trans Ind Electron* 55(11):3846–3854
- Mobayen S, Tchier F, Ragoub L (2017) Design of an adaptive tracker for n-link rigid robotic manipulators based on super-twisting global nonlinear sliding mode control. *Int J Syst Sci* 48(9):1990–2002
- Levant A (2003) Higher-order sliding modes, differentiation and output-feedback control. *Int J Control* 76(9–10):924–941
- Ming C, Gang C, Feijie H, Qingxuan J (2013) Active disturbance rejection control for trajectory tracking of manipulator joint with flexibility and friction. *Appl Mech Mater* 325–326: 1229–1232
- Hill J, Fahimi F (2011) Active disturbance rejection for bipedal walk of a humanoid using the motion of the arms. In: ASME 2011 International mechanical engineering congress and exposition, pp 137–144
- Poznyak A, Sánchez E, Wen Y (2001) Differential neural networks for robust nonlinear control (Identification, state estimation and trajectory tracking). World Scientific Press
- Peña GG, Consoni LJ, dos Santos WM, Siqueira AA (2019) Feasibility of an optimal emg-driven adaptive impedance control applied to an active knee orthosis, vol 112. [Online]. Available: <http://www.sciencedirect.com/science/article/pii/S0921889018304263>
- Cheah C-C, Wang D (1998) Learning impedance control for robotic manipulators. *IEEE Trans Robot Autom* 14(3):452–465
- Yongling F, Xu H, Sepehri N, Guozhe Z, Jian F, Liming Y, Rongrong Y (2018) Design and performance analysis of position-based impedance control for an electrohydrostatic actuation system. *Chin J Aeronaut* 31(3):584–596
- Hogan N (1987) Stable execution of contact tasks using impedance control. In: IEEE International conference on robotics and automation, pp 1047–1054
- Tucker MR, Olivier J, Pagel A, Bleuler H, Bouri M, Lamberty O, del Millán RJ, Riener R, Vallery H, Gassert R (2015) Control strategies for active lower extremity prosthetics and orthotics: a review. *J Neuroeng Rehabil* 12(1):1

36. Haddad WM, Chellaboina V (2008) Nonlinear dynamical systems and control. Princeton University Press
37. Moreno A, Osorio M (2012) Strict lyapunov funtions for the super-twisting algorithm. IEEE Tran Aut Cont 57(4):1035–1040
38. Salgado I, Chairez I, Camacho O, Yanez C (2014) Super-twisting sliding mode differentiation for improving pd controllers performance of second order systems. IS 53(4):1096–1106
39. Gao Z (2006) Active disturbance rejection control: a paradigm shift in feedback control system design. In: American control conference. Minneapolis, pp 2399–2405
40. Polyakov A, Chairez I (2014) A new homogeneous quasi-continuous second order sliding mode control. In: Proceedings of the XVI Latin American automatic control congress
41. Levant A (2007) Finite differences in homogeneous discontinuous control. IEEE Trans Autom Control 52(7):1208–1217

Publisher's note Springer Nature remains neutral with regard to jurisdictional claims in published maps and institutional affiliations.



M. Ballesteros-Escamilla received the M.Sc. degree in advance technologies from UPIITA IPN in 2015. She is enrolled in the PhD program in Automatic Control at CINVESTAV IPN. Her research interest includes robotics, adaptive programming, and robust control.



I. Salgado received the Ph.D. degree in computer sciences from Centro de Investigación en Computación-IPN. His current research interests include the design, control, and optimization of robotic systems and adaptive control.



I. Chairez received the Master's and Ph.D. degrees in control sciences from the Department of Automatic Control, CINVESTAV-IPN, 2004 and 2007. His research interests include neural networks, nonlinear control, and game theory.



D. Cruz-Ortiz is currently a Ph.D. student at the Automatic Control Department from the Advanced Studies and Research Center. His research interests include sliding mode control and robotic systems applied to muscle-skeletal rehabilitation.